 CMES, vol.17, no.1, pp.47-54, 2007

Cumulative Nonlinear Effects in Acoustic Wave Propagation

Ivan Christov[1], C.I. Christov[2] and P.M. Jordan[3]

Abstract: Two widely-used weakly-nonlinear models of acoustic wave propagation — the inviscid Kuznetsov equation (IKE) and the Lighthill–Westervelt equation (LWE) — are investigated numerically using a Godunov-type finite-difference scheme. A reformulation of the models as conservation laws is proposed, making it possible to use the numerical tools developed for the Euler equations to study the IKE and LWE, even after the time of shock-formation. It is shown that while the IKE is, without qualification, in very good agreement with the Euler equations, even near the time of shock formation, the same cannot generally be said for the LWE.

Keyword: Compressible flows, shock waves, nonlinear acoustics

1 Introduction

Singular surfaces are an important class of nonlinear wave phenomena. Physically, these surfaces represent propagating wavefronts, across which one or more quantities of interest suffer a jump discontinuity (or jump for short). What is most interesting about such nonlinear waves, in particular the subclass known as *acceleration waves*[1], is the fact that under certain conditions, even when the initial input is continuous, the jump amplitude can exhibit *finite-time blow-up*, also known as "gradient catastrophe" in the mathematical literature. The general study of acceleration waves has been, and remains, a topic of great interest in many areas of the physical sciences. This is especially true in the literature of continuum mechanics, where numerous works detailing cases of finite-time blow-up have appeared (see, *e.g.*, Coleman and Gurtin (1967); Chen (1973); McCarthy (1975); Elcrat (1977); Lindsay and Straughan (1978); Greenspan and Nadim (1993); Müller and Ruggeri (1993); Saccomandi (1994); Quintanilla and Straughan (2004) and the references therein]. To some researchers, blow-up of an acoustic acceleration wave's amplitude can only mean one thing: The formation of a *shock wave*, *i.e.*, a propagating jump in the velocity component perpendicular to the wavefront [Chen (1973)]. To others, however, this is an unproven conjecture [Coleman and Gurtin (1967); Fu and Scott (1991)]. A central question here is the following: What happens to the waveform *after* finite-time blow-up occurs?

The classical context for investigating the properties of acoustic acceleration waves is provided by the dynamic theory of lossless compressible fluids, the basis of which are the equations of Euler. In addition to the Euler equations, however, several weakly-nonlinear models also appear in the literature of this field. Of these, the Lighthill–Westervelt equation (LWE) and the inviscid Kuznetsov equation (IKE) are the best known. Yet, numerical studies of these (approximate) equations are scarce, as noted in the survey articles on nonlinear acoustics by Makarov and Ochmann (1996; 1997a,b). In fact, the only comparative (numerical) study of the latter models known to the present authors is that of Kagawa *et al.* (1992), who reported significant discrepancies between the solution of LWE and the reference solution for certain problems involving self-focusing apertures. Moreover, their results suggest that the IKE is a very good model of the exact

[1] Department of Mathematics, Texas A&M University, College Station, TX 77843-3368, USA

[2] Department of Mathematics, University of Louisiana at Lafayette, LA 70504-1010, USA

[3] Code 7181, Naval Research Laboratory, Stennis Space Center, MS 39529–5004, USA. E-mail: pjordan@nrlssc.navy.mil

[1] See the review articles by Chen (1973) and McCarthy (1975). Also, in some of the earlier works in the field, acoustic acceleration waves are referred to as "sonic discontinuities;" see, *e.g.*, Thomas (1957).

dynamics.

Expanding upon our work in Christov *et al.* (2006), we present an in-depth study of these weakly-nonlinear models by means of a Godunov-type numerical scheme and singular surface analysis. These techniques are applied to the Euler equations, IKE, and LWE alike. The results obtained are compared and contrasted in order to assess the range of applicability of each of the approximate models. We also briefly touch upon the question of what happens after finite-time blow-up occurs.

2 Governing equations

Consider a lossless compressible fluid, which is assumed to behave as a perfect gas [as defined on p. 79 of Thompson (1972)], that is initially in its equilibrium state. Assuming a homentropic flow, the equations of mass and momentum conservation, along with the polytropic equation of state, which we collectively refer to here as the Euler equations, are given by

$$\mathfrak{p}_t + \nabla\cdot(\mathfrak{p}\mathbf{v}) = 0, \tag{1}$$

$$\mathfrak{p}\left[\mathbf{v}_t + (\mathbf{v}\cdot\nabla)\mathbf{v}\right] + \nabla\wp = 0, \tag{2}$$

$$\wp = \wp_0(\mathfrak{p}/\mathfrak{p}_0)^\gamma, \tag{3}$$

respectively. Here, $\mathbf{v}$ is the velocity vector, $\mathfrak{p}(>0)$ is the mass density, $\wp(>0)$ is the thermodynamic pressure, the constant $\gamma(>1)$, which is known as the adiabatic index, is equal to the ratio of specific heats, and all body forces have been neglected. Moreover, by equilibrium state we mean the unperturbed, quiescent state in which $\wp=\wp_0$, $\mathfrak{p}=\mathfrak{p}_0$, $\eta=\eta_0$, and $\mathbf{v}=(0,0,0)$, where η is the specific entropy and $\wp_0$, $\mathfrak{p}_0$, and η_0 are constants. Additionally, we note that the assumption of homentropic flow means that $\eta_t+\mathbf{v}\cdot\nabla\eta=\nabla\eta=0$ for all $t\geq 0$ [see pp. 59–60 of Thompson (1972)].

Before proceeding to our numerical studies, we first review the conditions under which finite-time blow-up occurs. For simplicity, we limit our attention to one-dimensional (1D) flow along the x-axis, *i.e.*, a flow such that $\mathbf{v}=(u(x,t),0,0)$. Also, it should be noted that our presentation, which follows those given by a number of other authors [*e.g.*, Thomas (1957); Elcrat (1977)], is rooted in the theory of singular surfaces and is carried out on the exact, fully nonlinear (1D) Euler equations.

3 Acceleration wave analysis

Let us begin by considering a smooth planar surface $x=\Sigma(t)$ that is propagating along the x-axis of a Cartesian coordinate system in a region occupied by a perfect gas. Let the speed of Σ with respect to the gas immediately ahead of it be $U(>0)$. Here, following the usual convention, a "+" superscript denotes the region into which Σ is advancing and a "−" superscript denotes the region behind Σ. Furthermore, suppose that both u and $\mathfrak{p}$ are continuous functions of x and t, but that at least one of their first derivatives, say u_t, suffers a jump across Σ; *i.e.*, $[\![u]\!]=[\![\mathfrak{p}]\!]=0$, but $[\![u_t]\!]\neq 0$, where $[\![F]\!]\equiv F^- - F^+$ and for any function F we assume that $F^\mp \equiv \lim_{x\to\Sigma(t)^\mp} F(x,t)$ exist[2]. If $F^-\neq F^+$, then Σ is termed a singular surface with respect to F. In our particular case, $F=u_t$, hence Σ is classified as an acceleration wave [Chen (1973)]. Thus, given the above, and the value of $[\![u_t]\!]$ at $t=0$, the task now is to determine $[\![u_t]\!]$ for all later times.

A fundamental result of singular surface theory is known as Hadamard's lemma [see, *e.g.*, Chen (1973); McCarthy (1975); Bland (1988)]. For the problem at hand, Hadamard's lemma takes the form

$$\frac{\mathfrak{D}[\![F]\!]}{\mathfrak{D}t} = [\![F_t]\!] + V[\![F_x]\!], \tag{4}$$

where the 1D displacement derivative $\mathfrak{D}/\mathfrak{D}t$ gives the time-rate-of-change measured by an observer traveling with Σ and $V(\neq 0)$ denotes the velocity of Σ measured by an observer at rest. Now, since we have assumed $[\![u]\!]=[\![\mathfrak{p}]\!]=0$, then by Eq. (4) it follows that

$$V[\![u_x]\!] + [\![u_t]\!] = 0, \quad V[\![\mathfrak{p}_x]\!] + [\![\mathfrak{p}_t]\!] = 0. \tag{5}$$

Let us also take the jumps of Eqs. (1) and (2), which is permissible since they hold on both sides of Σ. After employing the formula for the jump of a product, $[\![\mathscr{A}\mathscr{B}]\!] = \mathscr{A}^+[\![\mathscr{B}]\!] + \mathscr{B}^+[\![\mathscr{A}]\!] +$

[2] We should note that F^+ and F^- are, at most, functions of t only.

$[\![\mathscr{A}]\!][\![\mathscr{B}]\!]$, and simplifying, we get the two additional jump relations

$$\begin{aligned} &[\![\mathfrak{p}_t]\!]+u^+[\![\mathfrak{p}_x]\!]+\mathfrak{p}^+[\![u_x]\!]=0,\\ &\mathfrak{p}^+[\![u_t]\!]+\mathfrak{p}^+u^+[\![u_x]\!]+\wp_{\mathfrak{p}}^+[\![\mathfrak{p}_x]\!]=0. \end{aligned} \tag{6}$$

Using Eqs. (5) and $(6)_1$, we can express the jumps in $\mathfrak{p}_x$, $\mathfrak{p}_t$, and u_x in terms of the jump in u_t. This yields, after simplifying and setting $A(t)\equiv[\![u_t]\!]$,

$$\begin{aligned} [\![u_x]\!] &= -V^{-1}A,\\ [\![\mathfrak{p}_t]\!] &= \frac{\mathfrak{p}^+}{V-u^+}A,\\ [\![\mathfrak{p}_x]\!] &= \frac{-\mathfrak{p}^+}{V(V-u^+)}A. \end{aligned} \tag{7}$$

Since $U>0$ by assumption, and $U=|V-u^+|$ by definition, it follows that $V\neq u^+$.

The next step is to determine V. Clearly, nonzero values of V that satisfy the above system of four jump equations, *i.e.* Eqs. (5) and (6), exist only if the determinant of the corresponding coefficient matrix is zero. This leads to the propagation condition $U^2=\wp_{\mathfrak{p}}^+$, and consequently the well known result

$$V=u^+\pm\sqrt{\wp_{\mathfrak{p}}^+}\,. \tag{8}$$

Henceforth, we will take Σ to be right-running, *i.e.*, we disregard the "$-$" case and assume $u^+\geq 0$.

Having determined the propagation velocity, the next step is to derive the equation governing $A(t)$. Although we omit the remaining details, it is a relatively straightforward, but rather lengthy, process using Hadamard's lemma, Eqs. (1) and (2), and the above jump relations to show that the jump amplitude satisfies the quadratic Bernoulli equation

$$\frac{\mathfrak{D}A}{\mathfrak{D}t}-\Lambda(t)A^2+\varkappa(t)A=0, \tag{9}$$

where

$$\begin{aligned} \Lambda(t) &= \frac{1}{V}\left(1+\frac{\mathfrak{p}^+\wp_{\mathfrak{pp}}^+}{2U^2}\right),\\ \varkappa(t) &= \frac{U\mathfrak{p}_x^+}{2\mathfrak{p}^+}-\frac{1}{2}\frac{\mathfrak{D}}{\mathfrak{D}t}\ln\left(\frac{U}{\mathfrak{p}^+}\right)-\frac{u_t^+-Vu_x^+}{V}\\ &\quad -\frac{\wp_{\mathfrak{pp}}^+\left(\mathfrak{p}_t^+-V\mathfrak{p}_x^+\right)}{2VU}+\frac{u_t^+-u^+u_x^+}{2U}. \end{aligned} \tag{10}$$

For definiteness, we further assume that the gas ahead of Σ is in its equilibrium state. Thus, $u^+=0$, $\mathfrak{p}^+=\mathfrak{p}_0$, $\wp_{\mathfrak{p}}^+=c_0^2$, and $\wp_{\mathfrak{pp}}^+=c_0^2(\gamma-1)/\mathfrak{p}_0$, where $c_0\equiv\sqrt{\gamma\wp_0/\mathfrak{p}_0}$ denotes the sound speed in the undisturbed gas. Consequently, $\varkappa(t)=0$, $\Lambda(t)=\Lambda_0\equiv c_0^{-1}(\gamma+1)/2$, and the jump amplitude solution is easily found to be

$$A(t)=\frac{A(0)}{1-\Lambda_0A(0)t}, \tag{11}$$

where $A(0)(\neq 0)$ denotes the value of A, *i.e.*, $[\![u_t]\!]$, at time $t=0$. According to Eq. (11), the evolution of $A(t)$ can be described, qualitatively, as follows:

(i) If $A(0)<0$ $\{\Rightarrow$ that Σ is expansive [see Chen (1973)]$\}$, then $A(t)\to 0$ from below as $t\to\infty$.

(ii) If $A(0)>0$ $\{\Rightarrow$ that Σ is compressive [see Chen (1973)]$\}$, then $\lim_{t\to t_\infty}A(t)=\infty$, where the breakdown time t_∞ is given by $t_\infty=[\Lambda_0A(0)]^{-1}$.

We note that contained in case (ii) are the conditions for finite-time blow-up.

4 Review of the model equations

As shown/noted in a number of works [see Christov *et al.* (2006) and the references therein], Eqs. (1)–(3) can be combined into a single equation for the velocity (or acoustic) potential ϕ, namely

$$\begin{aligned} &[1-\varepsilon(\gamma-1)\phi_t]\phi_{xx}-2\varepsilon\phi_x\phi_{tx}-\phi_{tt}\\ &\qquad =\tfrac{1}{2}\varepsilon^2(\gamma+1)(\phi_x)^2\phi_{xx}, \end{aligned} \tag{12}$$

where $\phi_x(x,t)=u(x,t)$ and $(0<)\varepsilon=u_0/c_0$ is the Mach number. Here, we note that Eq. (12), and all others henceforth, are expressed in terms of the following dimensionless variables:

$$\begin{aligned} \phi' &= \phi/(u_0x_0),\\ x' &= x/x_0,\\ t' &= t(c_0/x_0),\\ u' &= u/u_0,\\ \mathfrak{p}' &= \mathfrak{p}/\mathfrak{p}_0, \end{aligned} \tag{13}$$

where $u_0(>0)$ and $x_0(>0)$ denote a characteristic speed and length, respectively, and all primes have been omitted but are assumed understood.

Notice that if $\varepsilon \ll 1$, then the right-hand-side of Eq. (12) can be neglected to obtain a weakly-nonlinear approximation. However, in the literature, another weakly-nonlinear approximation is commonly used, which was first derived by Kuznetsov (1971) for thermoviscous gases. The lossless version of the latter, which we call the inviscid Kuznetsov equation (IKE), reads [see, *e.g.*, Naugolnykh and Ostrovsky (1998)]

$$\phi_{xx} - [1+\varepsilon(\gamma-1)\phi_t]\phi_{tt} = 2\varepsilon\phi_x\phi_{xt}. \tag{14}$$

In Christov *et al.* (2006), we showed how the IKE can be derived directly from Eq. (12) through a leading-order binomial series expansion in ε.

Another common weakly-nonlinear model can be derived from Eq. (14) by employing the linear-impedance assumption (LIA) $\phi_x \approx -\phi_t$ [Naugolnykh and Ostrovsky (1998); Christov *et al.* (2006)] on the right-hand (*i.e.*, the perturbing) side of Eq. (14) only. This yields the Lighthill–Westervelt equation (LWE):

$$\phi_{xx} - [1+\varepsilon(\gamma+1)\phi_t]\phi_{tt} = 0. \tag{15}$$

It should be noted that the LIA is exact for linear progressive (*e.g.*, harmonic) plane waves. Hence, it can be expected that the LIA is a reasonable approximation for motions that do not significantly deviate from the linear profile. It should also be noted that all three of our model equations yield the *same* expressions for $A(t)$ [see Eq. (11)] and t_∞.

5 Reformulation of the governing equations as conservation laws

In order to study the full range of applicability of the approximate models, we must be able to solve the equations numerically for times beyond the blow-up (or shock-formation) moment. To this end, we use the so-called MUSCL–Hancock scheme — a shock-capturing, upwind Godunov-type method, — which we have implemented as described in Christov *et al.* (2006). Note that such schemes can only be applied to conservation laws, and so we must reformulate the equations discussed above as such.

To this end, we begin by observing that the 1D Euler equations correspond to the following conservation law:

$$\begin{pmatrix} \mathfrak{p} \\ \mathfrak{p}u \end{pmatrix}_t + \begin{pmatrix} \varepsilon\mathfrak{p}u \\ \varepsilon\mathfrak{p}u^2 + \varepsilon^{-1}\mathfrak{p}^\gamma/\gamma \end{pmatrix}_x = 0. \tag{16}$$

To rewrite the weakly nonlinear potential equations as conservation laws, we begin with the well-known relations $u = \phi_x$ and $\mathfrak{p} - 1 = -\varepsilon\phi_t$. In the case of the IKE, this yields, as a preliminary step, the system

$$\begin{aligned} &\left[\varepsilon^2 u^2 - \gamma\mathfrak{p} + \tfrac{1}{2}(\gamma-1)\mathfrak{p}^2\right]_t - \varepsilon u_x = 0, \\ &u_t + \varepsilon^{-1}\mathfrak{p}_x = 0, \end{aligned} \tag{17}$$

which is not (yet) in the desired form. Next, we introduce the variable transformation:

$$\begin{aligned} &\tilde{\mathfrak{p}} = \gamma\mathfrak{p} - \tfrac{1}{2}(\gamma-1)\mathfrak{p}^2 - \varepsilon^2 u^2 \quad \Longleftrightarrow \\ &\mathfrak{p} = \frac{1}{\gamma-1}\left(\gamma \mp \sqrt{\gamma^2 - 2(\gamma-1)(\varepsilon^2 u^2 + \tilde{\mathfrak{p}})}\right). \end{aligned} \tag{18}$$

Here, we observe that for consistency, the "$-$" sign must selected so that $\mathfrak{p} \to 0$ when $\tilde{\mathfrak{p}}, u \to 0$. Now, rewriting Eq. (17) in terms of these new variable and simplifying, we obtain the following conservation law corresponding to the IKE:

$$\begin{pmatrix} \tilde{\mathfrak{p}} \\ u \end{pmatrix}_t + \begin{pmatrix} \varepsilon u \\ -[\varepsilon(\gamma-1)]^{-1}\sqrt{\gamma^2 - 2(\gamma-1)(\varepsilon^2 u^2 + \tilde{\mathfrak{p}})} \end{pmatrix}_x = 0. \tag{19}$$

Lastly, for completeness, we restate (in terms of the above parameters) the following conservation law corresponding to the LWE, which was derived in Christov *et al.* (2006) following a similar approach to the one used above for the IKE:

$$\begin{pmatrix} \tilde{\mathfrak{p}} \\ u \end{pmatrix}_t + \begin{pmatrix} \varepsilon u \\ -[\varepsilon(\gamma+1)]^{-1}\sqrt{(\gamma+2)^2 - 2(\gamma+1)\tilde{\mathfrak{p}}} \end{pmatrix}_x = 0, \tag{20}$$

where $\tilde{\mathfrak{p}} = (\gamma+2)\mathfrak{p} - \frac{1}{2}(\gamma+1)\mathfrak{p}^2$ in this case.

The derivation of conservation laws for the weakly nonlinear models was an essential step in our study because we may now apply a variety of advanced numerical solution techniques.

Because of its simplicity and efficiency, we have chosen the MUSCL–Hancock scheme. The latter is a second-order-accurate generalization of Godunov's scheme that allows us to simulate all three models (Euler, IKE, and LWE) using a unified approach. [For a recent higher-order generalization of such methods, applied to compressible MHD flows, see Balbás and Tadmor (2006).]

It should be noted that one could have also used the discontinuous Galerkin method [see, *e.g.*, Bargmann and Steinmann (2005) and the references therein] or the promising new technique, the so-called L^1-minimization FEM, which is especially effective in the case of (ill-posed) boundary-value problems [see Guermond and Popov (2007)].

6 Numerical results

In this section, we present and discuss numerical solutions of the conservation laws derived above subject to the initial conditions

$$\rho(x,0)=0, \quad u(x,0)=0, \tag{21}$$

and the boundary conditions (BC)

$$\left\{\begin{array}{ll}\text{(density BC)} & \rho(0,t)\\ \text{(velocity BC)} & \varepsilon u(0,t)\end{array}\right\} = [H(t)-H(t-t_w)]f(t), \tag{22}$$

where $H(\,\cdot\,)$ denotes the Heaviside unit step function and $\rho \equiv \mathfrak{p}-1$ is the dimensionless acoustic density or condensation. Recall that, initially, the medium is in its equilibrium state, as stated by Eqs. (21), and hence remains so ahead of Σ for all $t>0$. Furthermore, Eq. (22) states that a pulse of finite duration (or width) t_w is introduced at the boundary $x=0$, either in the density or velocity field, at time $t=0+$. In the simulations below, we assume the propagation medium to be air at 20°C, implying $\gamma=1.4$ and hence $t_\infty=1$ for a Mach number of $\varepsilon=0.26503$. We have also taken $t_w=1$ for the sake of simplicity.

In Fig. 1, we compare the solutions of the conservation laws corresponding to the Euler equations, the LWE, and the IKE with the linear wave equation solution. In addition, we have plotted the tangent line, as given by Eq. (11), at the wavefront to illustrate the amplitude of Σ.

The results in Fig. 1 show that the solution of the IKE remains very close to the solution of the Euler equations, while the solution of the LWE deviates from the latter as time advances. The discrepancy can be attributed to a saturation of the nonlinearity in the LWE [Christov *et al.* (2006)]; *i.e.*, the LIA changes the nature of the nonlinearity in the equations of motion. Moreover, it is interesting to note the dynamics of the LWE when a velocity BC is imposed — in particular, the much faster rate of steepening exhibited behind the wavefront. Even though the LWE retains the exact dynamics of Euler equations *at* the wavefront Σ, as can be verified analytically, it undesirably alters the profile *behind* Σ. Clearly, this shortcoming of the LWE stems directly from the use of the LIA because the IKE (in whose derivation the LIA is not used) does not exhibit the latter distortion. In a sense, the LIA alters *cumulative* nonlinear effects (*e.g.*, steepening and breaking) in the equations of motion, while retaining the *local* nonlinear effects (*e.g.*, finite-time blow-up at the wavefront Σ). Additionally, we observe that after the time of shock formation[3], all three nonlinear profiles show an increase in Σ's speed of propagation, with the LWE exhibiting the greatest increase. The agreement between the Euler and IKE profiles, while still good, has slightly deteriorated.

In Fig. 2, following the same color convention as Fig. 1, we present two measures of the error admitted by the approximate solutions as a function of time for the density BC. Here, we observe that the errors for the velocity BC are qualitatively the same but quantitatively larger. The left panel of Fig. 2 shows that there is a saturation of the error over time, which correlates well with the fact that the solution profiles eventually become vertical at Σ, at which point they are no longer changing with t. The most striking feature seen in the left panel, however, is that the error for LWE is consistently

[3] As noted on p. 402 of Thompson (1972), under the weakly-nonlinear approximation, small-amplitude shocks are very nearly isentropic; and thus a flow with weak shocks can still be treated as approximately homentropic.

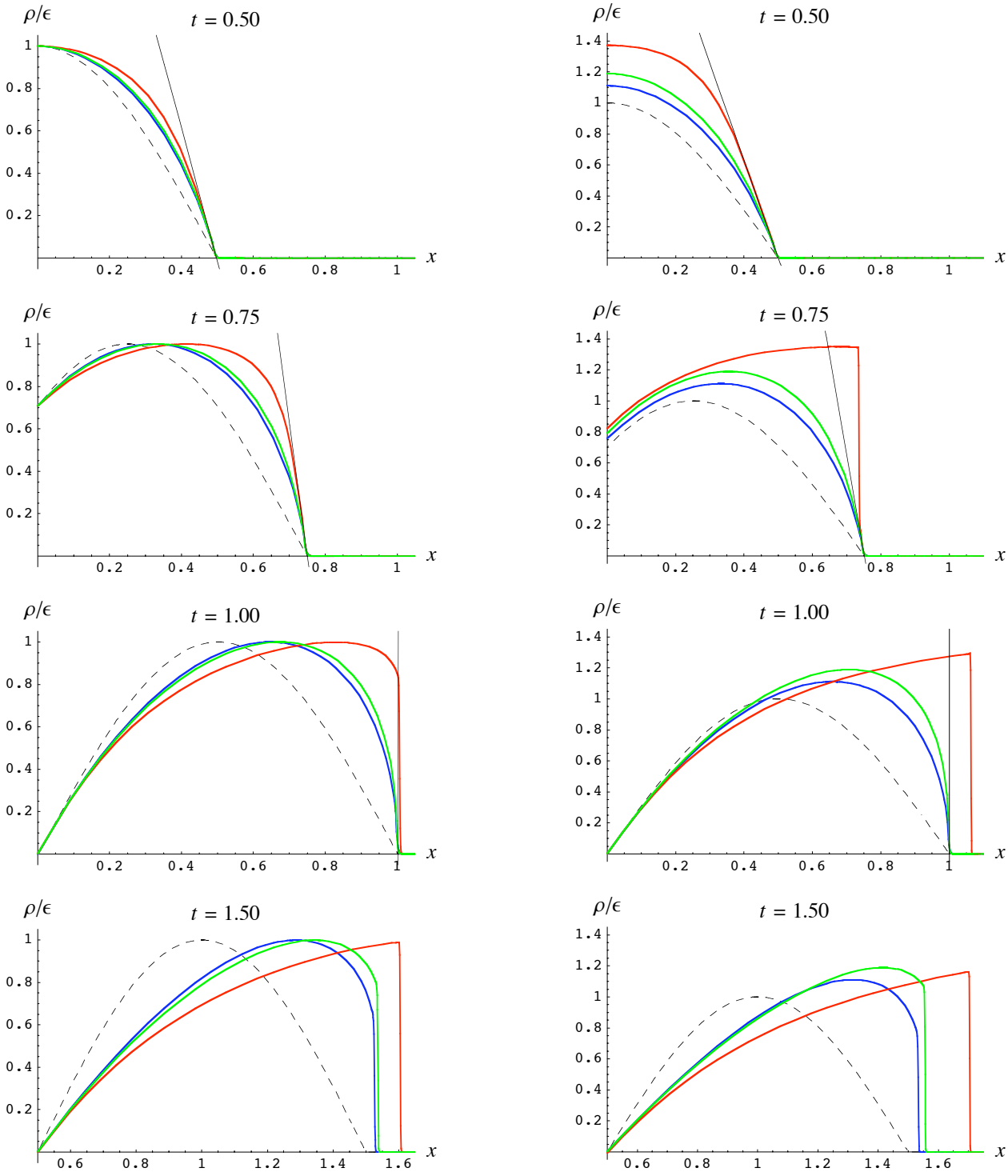

Figure 1: Eight snapshots in time (consecutively down each column) of the scaled dimensionless acoustic density, ρ/ε, vs. x for $f(t) = \varepsilon \sin(\pi t)$ with $\varepsilon = 0.26503$, and $t_\infty = 1$. The left column gives the density BC, and the right column shows the results for the velocity BC. The Euler equations, the LWE, and the IKE are in blue, red, and green, respectively. The solution of the linear wave equation is in dashed black. (Note that in the printed version "blue," "green" and "red" refer to the darkest, lightest and intermediate shade of gray present, respectively.)

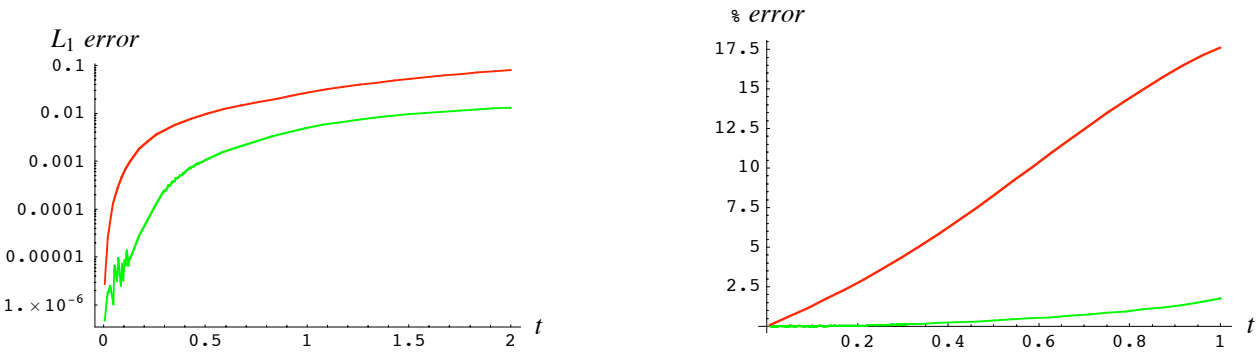

Figure 2: The left panel shows the growth of the L_1 norm of the difference between the exact (Euler) solution and the IKE and LWE solutions in log-linear scales, and the right panel shows in linear scales the growth of the maximal percentage error, as functions of time. The color convention is the same as that of Fig. 1.

an *order of magnitude* greater than the error for IKE, which further exemplifies the inadequacy of the LWE, and consequently use of the LIA in the nonlinear context.

In the right panel of Fig. 2 is shown the maximal percentage error. For the LWE, this quantity grows to about $10\times$ that of the IKE ($\approx$ 20% vs. 2%) prior to the time of shock formation, beyond which the percentage error is no longer a well-defined metric. Our results confirm the observation in Kagawa *et al.* (1992); *i.e.*, for certain problems, the solution of the LWE can be off by as much as 20%, while that of the IKE remains very close to the exact (Euler) one.

7 Conclusions

A comparative study of the two most common weakly-nonlinear approximations for compressible flow — the inviscid Kuznetsov equation (IKE) and the Lighthill–Westervelt Equation (LWE) — is presented. A novel reformulation of the IKE as a conservation law is discussed, extending the results for the LWE given in Christov *et al.* (2006). These reformulations enable us to employ a Godunov-type finite-difference scheme for the weakly-nonlinear equations in the same fashion as for the full Euler equations. By means of this powerful and extensible numerical tool, the evolution of the (compressive) waveform is examined for values of t well beyond t_∞, the instant of blow-up.

Our comparative numerical study reveals that the IKE approximates the exact (Euler) dynamics very well, even for relatively *large* values of t and ε, while the LWE is "crippled" due to the effects of the linear-impedance assumption (LIA) and proves to be an acceptable approximation to the Euler equations only for very small values of t and ε. In other words, when the LIA is employed, a significant degradation of the density profile is to be expected because the velocity (*i.e.*, ϕ_x) term is being replaced by one proportional to the density (*i.e.*, $-\phi_t$) in Eq. (14).

Additionally, we found that, for both the IKE and LWE models, the deviations from the full (Euler) model are considerably larger when the velocity BC, rather than the density BC, is imposed. The latter suggests that the effect of the nonlinearity is more pronounced when a nonuniform gas velocity is prescribed at the boundary.

Finally, as a follow-on to the present investigation, it may be worthwhile to compare the IKE with the approximate equation obtained by dropping the right-hand side of Eq. (12). We hope to address this and related issues in a future article.

Acknowledgement: C.I.C. was supported, in part, by an ASEE/ONR Summer Faculty Fellowship at the U. S. Naval Research Laboratory, Stennis Space Center, Mississippi. P.M.J. was supported by ONR/NRL funding (PE 061153N). All figures appearing in this article were generated using the software package MATHEMATICA (Version 5.2).

References

Balbás, J.; Tadmor, E. (2006): Nonoscillatory central schemes for one- and two-dimensional magnetohydrodynamic equations. II: Higher-order semidiscrete schemes. *SIAM J Sci Comput*, vol. 28, pp. 533–560.

Bargmann, S.; Steinmann, P. (2005): Finite element approach to non-classical heat conduction. *CMES: Computer Modeling in Engineering & Sciences*, vol. 9, pp. 133–150.

Bland, D. R. (1988): *Wave theory and applications.* Oxford University Press, Oxford, U.K.

Chen, P. J. (1973): Growth and decay of waves in solids. In: S. Flügge and C. Truesdell (eds) *Handbuch der physik*, Springer, Berlin, vol. VIa/3, pp. 303–402.

Christov, I.; Jordan, P. M.; Christov, C. I. (2006): Nonlinear acoustic propagation in homentropic perfect gases: A numerical study. *Phys Lett A*, vol. 353, pp. 273–280.

Coleman, B. D.; Gurtin, M. E. (1967): Growth and decay of discontinuities in fluids with internal state variables. *Phys Fluids*, vol. 10, pp. 1454–1458.

Elcrat, A. R. (1977): On the propagation of sonic discontinuities in the unsteady flow of a perfect gas. *Int J Eng Sci*, vol. 15, pp. 29–34.

Fu, Y. B.; Scott, N. H. (1991): The transition from acceleration wave to shock wave. *Int J Eng Sci*, vol. 29, pp. 617–624.

Greenspan, H. P.; Nadim, A. (1993): On sonoluminescence of an oscillating gas bubble. *Phys Fluids A*, vol. 5, pp. 1065–1067.

Guermond, J.-L.; Popov, B. (2007): Linear advection with ill-posed boundary condition via L^1-minimization. *Int J Num Anal Modeling*, vol. 4, pp. 39–47.

Jordan, P. M.; Christov, C. I. (2005): A simple finite difference scheme for modeling the finite-time blow-up of acoustic acceleration waves. *J Sound Vib*, vol. 281, pp. 1207–1216.

Kagawa, Y.; Tsuchiya, T.; Yamabuchi, T.; Kawabe, H.; Fuji, T. (1992): Finite element simulation of non-linear sound propagation. *J Sound Vib*, vol. 154, pp. 125–145.

Kuznetsov, V. P. (1971): Equations of nonlinear acoustics. *Sov Phys Acoust*, vol. 16, pp. 467–470.

Lindsay, K. A.; Straughan, B. (1978): Acceleration waves and second sound in a perfect fluid. *Arch Rat Mech Anal*, vol. 68, pp. 53–87.

Makarov, S.; Ochmann, M. (1996): Nonlinear and thermoviscous phenomena in acoustics, Part I. *Acustica*, vol. 82, pp. 579–606.

Makarov, S.; Ochmann, M. (1997a): Nonlinear and thermoviscous phenomena in acoustics, Part II. *Acustica*, vol. 83, pp. 197–222.

Makarov, S.; Ochmann, M. (1997b): Nonlinear and thermoviscous phenomena in acoustics, Part III. *Acustica*, vol. 83, pp. 827–846.

McCarthy, M. F. (1975): Singular surfaces and waves. In: A. C. Eringen (ed) *Continuum physics*, Academic Press, London, vol. II, pp. 449–521.

Müller, I.; Ruggeri, T. (1993): Extended thermodynamics. In: C. Truesdell (ed) *Springer tracts in natural philosophy*, Springer, New York, vol. 37, pp. 148–152.

Naugolnykh, K.; Ostrovsky, L. (1998): *Nonlinear wave processes in acoustics*, Cambridge University Press, New York, Sect. 1.

Quintanilla, R.; Straughan, B. (2004): A note on discontinuity waves in type III thermoelasticity. *Proc R Soc A*, vol. 460, pp. 1169–1175.

Saccomandi, G. (1994): Acceleration waves in a thermo-microstretch fluid. *Int J Non-Linear Mech*, vol. 29, pp. 809–817.

Thomas, T. Y. (1957): The growth and decay of sonic discontinuities in ideal gases. *J Math Mech*, vol. 6, pp. 455–469.

Thompson, P. A. (1972): *Compressible-fluid dynamics.* McGraw–Hill, New York.